TRANSVERSE IMPEDANCE OF SINGLE FROG SKELETAL MUSCLE FIBERS

BERT A. MOBLEY
Department of Physiology and Biophysics, University of Oklahoma College of Medicine, Oklahoma City, Oklahoma 73190

G. EIDT
Mucina Manufacturing Company, Detroit, Michigan 48240

ABSTRACT The transverse electrical impedance of single frog skeletal muscle fibers was measured at 31 frequencies that ranged from 1 to 100,000 Hz. Each fiber was bathed entirely in Ringer's solution, but it was positioned so that a central length of 5 mm was in a hollow plastic disk and was electrically isolated from the ends of the fiber. The diameter of the segment of the fiber in the disk was measured and then the segment was pressed from opposite sides by two insulating wedges. Electrical current was passed transversely through the segment between two platinum-platinum black electrodes that were located in the pools of Ringer's solution within the disk. The results were corrected for stray parallel capacitance, series resistance of the Ringer's solution between the fiber and the electrodes, parallel shunt resistance around the fiber, and the phase shift of the measuring apparatus. A nonlinear least-squares routine was used to fit a lumped equivalent circuit to the data from six fibers. The equivalent circuit that was chosen for the fibers contained three parallel branches; each branch was composed of a resistor and a capacitor in series. The model also included a seventh adjustable parameter that was designed to account for the degree of compression of the fibers by the insulating wedges. The branches of the equivalent circuit were assumed to represent the electrical properties of: (*a*) the myoplasm in series with the membrane capacitance that was exposed directly to the pools of Ringer's solution; (*b*) the capacitance and series resistance of the transverse tubules that were exposed directly to the pools of Ringer's solution; (*c*) the membrane capacitance in series with the shunt resistance between the fibers and the insulating wedges. The results gave no indication that current entered the sarcoplasmic reticulum.

INTRODUCTION

Fatt (1964) measured the transverse impedance in sartorius muscles of frogs. He used extracellular electrodes and measured the impedance over the range of frequencies 1.5–130,000 Hz. The equivalent circuit or electrical model he fit to his data contained two parallel branches, and each branch contained a resistor and a capacitor in series. The resistor and capacitor that had the smaller time constant were assumed to reflect the resistivity of the myoplasm and the specific capacitance of the sarcolemma, respectively. The capacitor in the branch with the larger time constant averaged 54 μF per square centimeter of assumed sarcolemmal surface area. Assuming that the membranes of sarcoplasmic reticulum are like other biological membranes and have a specific capacitance of $\sim$1 μF/cm^2 (Cole, 1968), the larger capacitance in Fatt's model could have been caused in large part by the membranes of the sarcoplasmic reticulum, because the sarcoplasmic reticulum in frog fibers of $\sim$100 μm in diameter has been shown to have a surface area of $\sim$50 times the surface area of the sarcolemma (Peachey, 1965; Mobley and Eisenberg, 1975).

Experiments in which microelectrodes were used to measure input and transfer impedance of frog muscle fibers showed no evidence that passive electrical current entered the sarcoplasmic reticulum, but those results were consistent with the idea that passive electrical current charged the capacitances of the membranes of the sarcolemma and the transverse tubular system (Falk and Fatt, 1964; Freygang et al., 1967; Schneider, 1970; and Valdiosera et al., 1974*b*). Other experiments in which the longitudinal impedance of single frog muscle fibers was measured with extracellular electrodes showed similar negative results regarding the entry of current into the sarcoplasmic reticulum (Mobley et al., 1975). We measured the transverse impedance of single muscle fibers of frogs from 1 to 100,000 Hz using extracellular electrodes, and we used nonlinear curve fitting to see if the results of Fatt (1964) would be obtained.

METHODS

Mounting the Single Fibers

Single fibers were isolated from the dorsal head of the semitendinosus muscle of frogs, *Rana pipiens*. The dissection was carried out in a

Ringer's solution (113.5 mM NaCl, 2.5 mM KCl, 2.0 mM $CaCl_2$, 5.0 mM imidazole, 10.0 mM glucose, pH = 7.2) at 25°C. After each dissection, a single fiber was placed in a chamber that contained either Ringer's solution or a solution of low conductivity (198.5 mM sucrose, 2.5 mM KCl, 2.0 mM $CaCl_2$, 5.0 mM imidazole, 10.0 mM glucose, pH = 7.2) at 25°C.

The chamber also contained a hollow disk 5.2 cm in diameter and 5 mm high inside (see Fig. 1), which was filled with the same solution that was in the chamber. The upper and lower walls of the disk were each 2 mm thick. Holes 635 μm in diameter were drilled in the centers of the upper and lower walls, and silicone rubber was packed into the holes, leaving hollow cylinders 127 μm in diameter in the centers. Plastic cylinders whose inside diameters were 1 mm were centered and fixed above and below the upper and lower walls of the disk. The latter cylinders were 7 and 2 mm in length, respectively. One end of the fiber was pulled through the cylinders in the bottom of the disk first, then into the disk, and finally into the cylinders in the top of the disk. The solution in the chamber bathed the segment of the fiber that hung below the disk, and the solution in the upper cylinder (1 mm in diameter) bathed the segment of the fiber that extended above the disk. The pools of solution that bathed the upper segment of the fiber, the central segment of the fiber, 5 mm in length, and the lower segment of the fiber were not connected to each other except through the holes in the top and bottom of the disk.

The disk also contained two plastic wedges that were pressed against opposite sides of the central segment of the fiber. The parallel faces of the wedges that touched the fiber were coated with silicone rubber. When the wedges pressed against the fiber they insulated it on each side so that when electrical current was passed between two platinum-platinum black electrodes also located in the disk, much of the current passed transversely through the single fiber. A grounded shield was embedded in each wedge. The shields were composed of brass and they inserted into the brass rods (not shown in Fig. 1) that were used to control the position of the wedges. Neither the shields nor the rods came in contact with any of the pools of solution, and tests showed that no resistive current passed between the electrodes and the shields or rods. The ends of the shields were covered by the silicone rubber that coated the ends of the wedges. The coating of silicone rubber was 5 mm high, 750 μm wide, and 100 μm thick.

Electronic Apparatus

Fig. 1 illustrates a fiber mounted in the disk and chamber, and it also shows schematically the electronic apparatus that was used to measure the transverse impedance. The impedance was measured at 31 frequencies between 1 and 100,000 Hz (six frequencies per decade). After the measurement at 100,000 Hz, a second measurement was taken at 40 Hz for the purpose of checking the drift of the phase angle during the experiment. The drift of the phase angle was checked at 40 Hz instead of a lower frequency because the phase angles at frequencies <40 Hz were very close to zero. At each frequency, the applied voltage (RMS) and the DC voltages that were functions of the in phase and quadrature components of the current were measured and stored on a floppy disk in the computer. After an experiment, the magnitude and phase angle of the impedance were calculated at all 31 frequencies.

The oscillator was an Krohn-Hite-4001AR (Krohn-Hite Corp., Avon, MA); the rms (root mean square) converter was a modified Data Precision digital voltmeter; the current amplifier was a Teledyne Philbrick 1027 operational amplifier with 10,000 Ω and 10 pF in the feedback loop; the lock-in amplifier was a Princeton 129A (Princeton Gamma-Tech, Inc. Princeton, NJ); the three DC amplifiers were three AD517 precision IC operational amplifiers (Analog Devices, Inc., Norwood, MA); and the computer was an 11/03 (Digital Equipment Corp. Marlboro, MA) with an A-D converter.

The maximum current applied to any fiber was 8.6×10^{-9} A, which occurred at high frequencies. The current that was passed at low frequencies was <10% of the maximum current for that fiber. Consider-

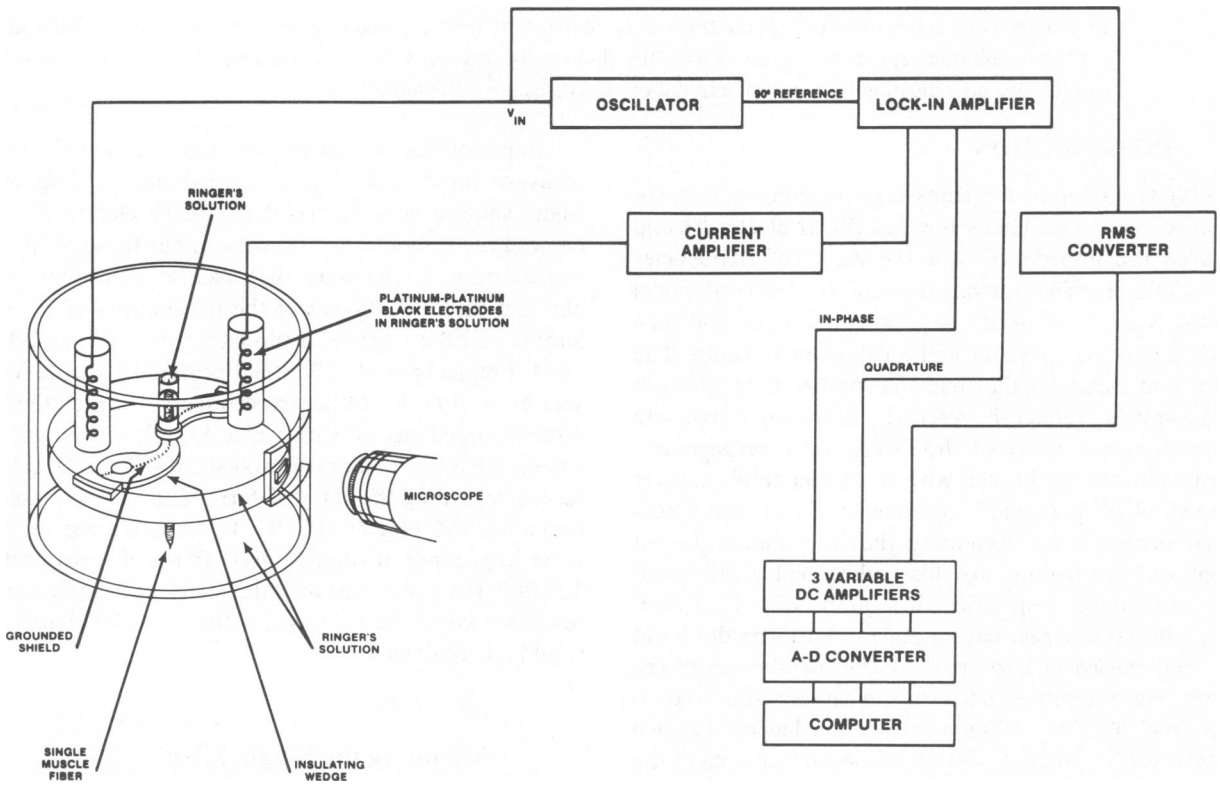

FIGURE 1 A schematic diagram of a single fiber mounted in the disk and chamber. The electronic apparatus that was used to measure the transverse impedance is also illustrated. V_{in} and the output voltage from the current amplifier were monitored on an oscilloscope.

ing the magnitude of the shunt around the fiber and the magnitude of the current, the membrane potential of any fiber was probably never altered by as much as 1 mV.

Equivalent Circuit and Curve Fitting

At the beginning of an experiment, the diameter (Diam) of the fiber was measured and then the wedges were pressed against the fiber. We attempted to make the shunt impedance around the fiber very large so that the specific membrane resistance could be measured accurately. However, that proved to be impossible with our apparatus, and *RP* (Fig. 2) was chosen to represent the shunt resistance in parallel with a series combination of membrane and myoplasmic resistances. The wedges were pressed against the fiber until the magnitude of the quadrature component of current at 10,000 Hz began to decline; further pressure on the fiber invariably destroyed it. When the shunt resistance was as large as we could obtain for a given fiber, it was not possible to measure the width of the slit between the faces of the wedges. Either there was insufficient light coming through the fiber and slit, or the light coming through the silicone rubber on the faces of the wedges caused distortion of the light coming through the slit, or the angle of the faces of the wedges with respect to the line of sight into the disk was such that the fiber could not be seen. The segments of the fibers in the disk were observed to be in a flattened condition when the wedges were moved away from the fibers after an experiment. Obviously, the normal circular or elliptical cross section of the fibers was greatly distorted due to the compression by the wedges, and this was an important factor in the analysis of the results. Data from a fiber were considered acceptable if at the conclusion of an experiment, when the wedges were moved away from the fiber, no regions of contracture were observed.

Fig. 2 shows an equivalent circuit of the fiber and chamber. *CP* was the stray parallel capacitance of the experimental chamber; it was measured when the wedges were touching each other in the center of the disk and no fiber was in the disk (2.07 pF). Under those conditions the phase angle was ~90°.

RS was the series resistance that was caused by the bathing solution between the electrodes, which were 4.2 cm apart; it was measured when no fiber was mounted in the disk and the separation between the faces of the wedges was ~100 μm (3,905 Ω for Ringer's solution and 42,420 Ω for the low-conductivity solution). Probably the major contributor to RS during an experiment was the part of the slit, 750 μm long and 5 mm high, that was formed at the ends of the wedges and that did not contain the fiber. An accurate measurement of *RS* would be obtained if a fiber were removed from between the wedges and if, in addition, the space previously occupied by the fiber could be removed also. Obviously, an accurate measurement of *RS* in our apparatus could not be obtained. As noted in the preceding paragraph, we could not measure the separation of the wedges during an experiment, and even if we had been able to do so, a measurement of resistance at that separation of the wedges would have been larger than the true *RS*. Our method of measuring *RS*, which was admittedly inadequate, was to measure the resistance between the electrodes when no fiber was mounted and the separation of the wedges was approximately equal to the diameter of an uncompressed fiber.

RP was the combination of shunt resistance in parallel with the membrane and myoplasmic resistances; its magnitude was taken to be the largest resistance that was measured at any frequency after the data had been corrected for *CP*, *RS*, and the phase shift of the instrumentation. The phase shift of the instrumentation ranged between 0° at several frequencies in the midrange up to 3.3° at 1 Hz and up to 1.7° at 50,000 Hz in the high-frequency range.

Six elements, *RI*, *CM*, *RT*, *CT*, *RW*, and *CW*, of a lumped equivalent circuit (Fig. 2) plus a seventh parameter, *S*, (see Fig. 3) were fit to the data that were corrected for *CP*, *RS*, and instrumental phase shift. The fitting was accomplished by a nonlinear least-squares curve-fitting routine using a Levinberg-Marquardt algorithm (Valdiosera et al., 1974*a*; and Clausen et al., 1979). *RP* was held constant at its measured value during the fitting process.

The significance of the seventh adjustable parameter, *S*, is shown in Fig. 3. We assumed that the free central segment of each fiber had a circular cross section with the diameter, Diam, as measured (Fig. 3 *a*). Each fiber was then modeled as having a square cross section (Fig. 3 *b*) with a perimeter, 4*L*, that was equal to the circumference of the circular fiber, $\pi \cdot$(Diam), and therefore had a surface area equal to the surface area of the circular fiber. Fig. 3 *c* shows a square-fiber model compressed by the insulating wedges into a rectangle that has the same surface area as the square and circular fibers. As the distance between the faces of the insulating wedges was decreased, the surface area that was exposed directly to bathing solution was decreased by the factor $(1 - S)$ and the fraction of surface area touching the wedges was increased by the factor $(1 + S)$. The parameter *S* could range from 0 to 1; it expressed the degree of compression of the fiber. The computer chose the value of the parameter *S*, as well as *CM*, *RI*, *RT*, *CT*, *RW*, and *CW* that gave the best fit to the data.

The total impedance (Ω) of the equivalent circuit of the fiber that was

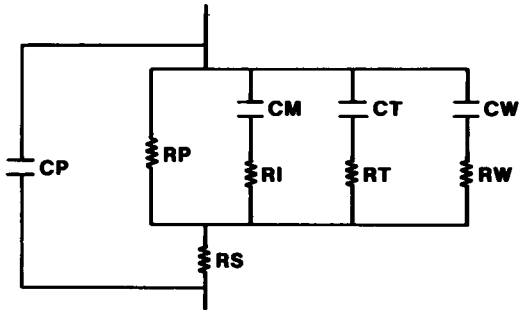

FIGURE 2 The lumped equivalent circuit that was chosen to represent the muscle fibers and the experimental disk and chamber. *CP* was the stray capacitance. *RS* was the series resistance of the bathing solution. *RP* was the combination of the shunt resistance around the fiber segments that was in parallel with a series combination of membrane resistance and myoplasmic resistance. The experimental data were corrected for the measured quantities, *CP*, *RS*, and the phase shift of the electronic apparatus, before the computer fitting occurred. During the fitting process, *RP*, which was also measured, was held constant. The predictions of phase angles from this model were compared with the measured phase angles that were corrected for instrumental phase shift.

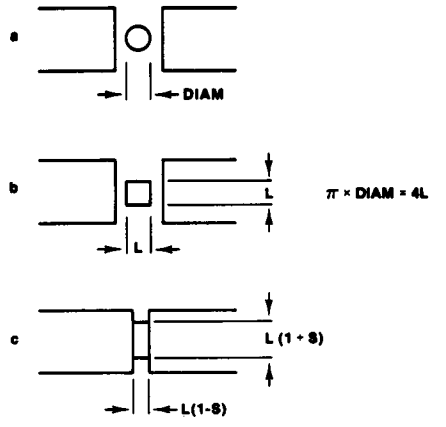

FIGURE 3 A top view of the model that was designed to account for the compression of the fiber segments by the insulating wedges. The three model fibers of circular, square, and rectangular cross section all had the same surface area. The parameter *S* was indicative of the degree of compression of the segments. The mean diameter of the fibers before compression was 96 μm. The actual length of the faces on the insulating wedges was 750 μm.

contained in Fig. 2 was $Z_{total} = 1/(1/Z_M + 1/Z_T + 1/Z_W)$, where

$$ZM = 2(\text{cm}^{-1}) \cdot RI(\Omega\,\text{cm}) \cdot \left(\frac{1+S}{1-S}\right) - \frac{16(\text{cm}^{-1})j}{\omega \cdot \pi \cdot \text{Diam(cm)} \cdot CM(\text{F/cm}^2) \cdot (1-S)},$$

$$ZT = 2(\text{cm}^{-1}) \cdot RT(\Omega\,\text{cm}) \cdot \left(\frac{1+S}{1-S}\right) - \frac{16(\text{cm}^{-1})j}{\omega \cdot \pi \cdot \text{Diam(cm)} \cdot CT(\text{F/cm}^2) \cdot (1-S)},$$

$$ZW = 2(\text{cm}^{-1}) \cdot RW(\Omega\,\text{cm}) \cdot \left(\frac{1+S}{1-S}\right) - \frac{16(\text{cm}^{-1})j}{\omega \cdot \pi \cdot \text{Diam(cm)} \cdot CW(\text{F/cm}^2) \cdot (1-S)},$$

$\omega = 2\pi f$, and f is the frequency.

RI, *RT*, and *RW* were resistivities of the fibers (Ω cm) in the real components of the impedances *ZM*, *ZT*, and *ZW*. The multiplicative factors of 2 in the real components were caused by the fact that the lengths of the segments that were investigated were 0.5 cm. The factor $(1 + S)$ was a component of the length of the transverse path of current through the fibers, and the factor $(1 - S)$ was a component of the width of the fibers through which the transverse current passed. *CM*, *CT*, and *CW* were specific capacitances (F/cm²) in the imaginary components of the impedances *ZM*, *ZT*, and *ZW*. Each side of the square, *L*, in Fig. 3 is equal to $\pi \cdot (\text{Diam})/4$ and was a component of the surface area of the fiber model. Each imaginary component of *ZM*, *ZT*, and *ZW* was modified by the factor $(1 - S)$ when the fiber was compressed by the wedges. In addition, one factor of 0.5 was caused by the fact that the length of each segment was 0.5 cm (the length of each segment was also a component of the surface area of the model). A second factor of 0.5 was caused by the fact that transverse current passed through two sections of surface membrane; and as Fig. 3 indicates, the two sections were assumed to be equal in area.

Theoretical Curves

Finally all parameters in Fig. 2 plus the parameter *S* were used to calculate the impedance of each fiber and the experimental chamber at all 31 experimental frequencies. A plot of phase angle with respect to frequency from the model was compared with the raw experimental data, i.e., the data that were corrected for instrumental phase shift.

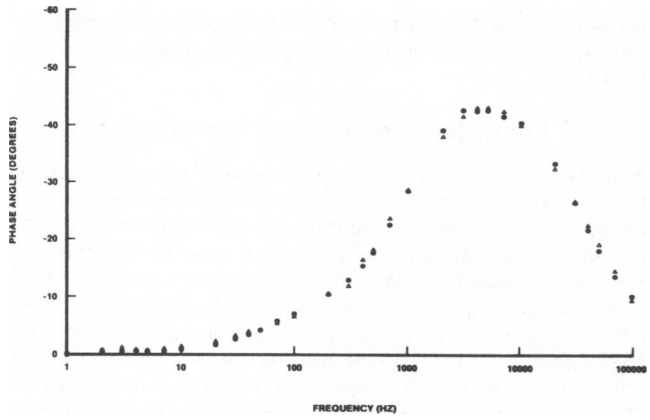

FIGURE 4 A plot of phase angle with respect to frequency for one of the fibers (fiber 1, Table I) that was mounted in the chamber and was bathed in Ringer's solution. The open triangles represent the measured data corrected for instrumental phase shift. The filled circles represent the best fit to the data by the lumped equivalent circuit in Fig. 2.

RESULTS

Data and Equivalent Circuit for Fibers in Ringer's Solution

Fig. 4 shows a plot of phase angle with respect to frequency for a fiber that was mounted in the chamber and was bathed in Ringer's solution. The open triangles represent the measured data corrected for instrumental phase shift, and the filled circles represent the best fit to the data by the lumped equivalent circuit shown in Fig. 2. The six circuit parameters for this fiber along with the parameter *S* (see Methods) which fit the data best, are listed in Table I as data from fiber 1. Other forms of an equivalent circuit could have been chosen and fit to the data, but the circuit in Fig. 2 was chosen because it is consistent with what is known about the physical structure of the muscle fibers and the apparatus and because it incorporated the equivalent circuit of muscle fibers that was used by Fatt (1964) on sartorius muscle.

TABLE I
PARAMETERS OF AN EQUIVALENT CIRCUIT OF SINGLE MUSCLE FIBERS

Fiber	Diameter*	*RI*	*CM*‡	*RT*	*CT*‡	*RW*	*CW*‡	*S*	*RP**
	(microns)	*(Ω cm)*	*(μF/cm²)*	*(Ω cm)*	*(μF/cm²)*	*(Ω cm)*	*(μF/cm²)*		*(Ω)*
1	*88*	*249*	*2.404*	*30,450*	*5.640*	*2,761*	*2.045*	*0.757*	*61,630*
2	*101*	*190*	*2.209*	*18,110*	*6.798*	*1,736*	*2.113*	*0.724*	*59,360*
3	*86*	*238*	*1.971*	*37,770*	*2.442*	*3,413*	*1.512*	*0.673*	*78,870*
4	*108*	*204*	*2.051*	*23,230*	*1.439*	*3,345*	*0.746*	*0.660*	*21,480*
5	*83*	*189*	*2.210*	*22,760*	*3.753*	*4,485*	*0.757*	*0.510*	*15,160*
6	*112*	*237*	*2.482*	*10,770*	*7.909*	*1,907*	*2.407*	*0.843*	*122,300*
Mean	*96*	*218*	*2.221*	*23,848*	*4.664*	*2,941*	*1.597*	*0.695*	*59,800*
SD	*12*	*27*	*0.197*	*9,412*	*2.538*	*1,032*	*0.716*	*0.112*	*39,331*
SEM	*5*	*11*	*0.080*	*3,842*	*1.036*	*421*	*0.292*	*0.046*	*16,057*

**Diameter and RP were measured quantities.*

‡*Referred to the surface area of the part of the segments that was directly exposed to the Ringer's solution.*

It is not obvious from Fig. 4 that a fiber model with three time constants was required for a good fit. We also fit our data with equivalent circuits having one branch (*RI*, *CM*, see Fig. 5) and two branches (*RI*, *CM* and *RW*, *CW*; see Fig. 6). A comparison of the fits of the data in Figs. 4–6 provides better evidence for an equivalent circuit with three time constants than plots of impedance loci of the fibers would provide.

Table I gives data for six single fibers that were bathed in Ringer's solution. Diam and *RP* were measured quantities; Diam was the diameter of the fiber before it was compressed by the wedges. *RP* was assumed to be the combination of shunt resistance in parallel with the series combination of membrane and myoplasmic resistances. *RP* was chosen as the largest resistance in the entire low-frequency range after the data were corrected for *CP* and *RS* (Fig. 2) and instrumental phase shift. The magnitude of *RP* was chosen in this manner rather than as the resistance at 1 Hz because five of the fibers showed a significant increase in resistance with frequency at low frequencies; fiber 2 in Table I was the exception. We assumed that at times the shunt resistance increased after the fibers were mounted and the experiments were begun. Our evidence for this assumption is not conclusive because the equivalent circuit is not a single resistor and capacitor; however, the measurements of impedance at 40 Hz on each fiber that was described in the Methods showed that in the interim (~15 min) between the first and second recordings of impedance at 40 Hz, the real part of the impedance increased in all fibers except in fiber 2 (fiber 1, +1%; fiber 2, −3%; fiber 3, +6%; fiber 4, +39%; fiber 5, +25%; fiber 6, +13%).

There was no measurement of drift in the fibers and experimental apparatus at the 10 frequencies between 1 and 40 Hz, and the total time required to make the 10 measurements at low frequencies was ~15 min. Although

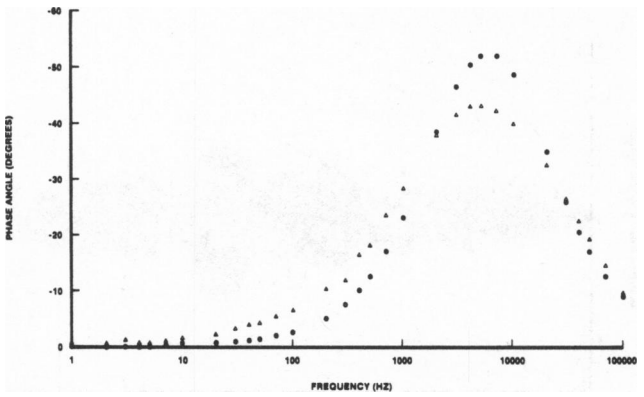

FIGURE 5 A plot of phase angle with respect to frequency for the fiber in Fig. 4. The open triangles represent the measured data corrected for instrumental phase shift. The filled circles represent the best fit to the data by the equivalent circuit in Fig. 2 without the circuit parameters *RW*, *CW*, *RT*, and *CT*. *RI* = 345 Ω cm, *CM* = 2.383 μF/cm², and *S* = 0.706.

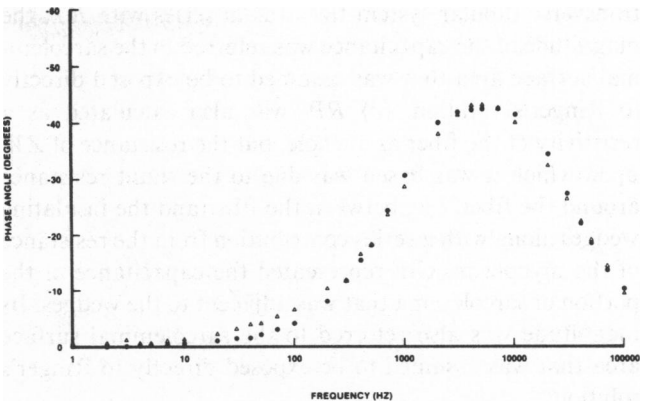

FIGURE 6 A plot of phase angle with respect to frequency for the fiber in Fig. 4. The open triangles represent the measured data corrected for instrumental phase shift. The filled circles represent the best fit to the data by the equivalent circuit in Fig. 2 without the circuit parameters *RT* and *CT*. *RI* = 155 Ω cm, *CM* = 3.811 μF/cm², *RW* = 2,062 Ω cm, *CW* = 3.525 μF/cm², and *S* = 0.847.

the large amount of drift in fibers 4 and 5 was of concern to us, the effect of the drift on the curve fitting was probably not significant because those two fibers experienced significant shunting (see *RP* in Table I), and so the phase angle was very small at 40 Hz. The drift in phase angle in degrees (negative) for all fibers at 40 Hz was: fiber 1, 3.8–3.0; fiber 2, 5.0–4.9; fiber 3, 4.0–4.3; fiber 4, 1.1–1.5; fiber 5, 1.2–1.7; fiber 6, 10.0–10.3; all changes were <1°. There was no indication that nonlinearities occurred, even when signals much larger than usual were applied.

The seven parameters, *RI*, *CM*, *RT*, *CT*, *RW*, *CW*, and *S*, were chosen by the computer to give the best fit to the experimental data. It is important to note that the parameter *S* represented the degree of compression of the fiber by the wedges, and the factor (1 − *S*) determined the fraction of the sarcolemma that was exposed directly to Ringer's solution. It is also important to note that if some circuit parameters are interpreted as representing the electrical properties of membranous structures within the volumes of the fibers, an implicit assumption is that the parameter (1 − *S*) controlled or limited the current to a proportional fraction of the total number or surface area of those structures.

Based upon the magnitudes of the parameters, the known structure of muscle fibers, the structure of the experimental apparatus, and the results of other studies, we propose that: (*a*) the parameter *RI* represented the resistivity of the myoplasm and *CM* represented the specific capacitance of the fraction of the sarcolemma that was assumed to be exposed directly to Ringer's solution. (*b*) *RT* was calculated as a resistivity of the fiber as a whole but the resistance of *ZT* upon which it was based was due to the lumen of the transverse tubular system that was exposed directly to Ringer's solution along with a small series contribution from the resistance of the myoplasm. *CT* represented the specific capacitance of the

transverse tubular system that was in series with *RT*; the magnitude of the capacitance was referred to the sarcolemmal surface area that was assumed to be exposed directly to Ringer's solution. (*c*) *RW* was also calculated as a resistivity of the fiber as a whole, but the resistance of *ZW* upon which it was based was due to the shunt resistance around the fiber, i.e., between the fiber and the insulating wedges along with a series contribution from the resistance of the myoplasm. *CW* represented the capacitance of the portion of sarcolemma that was adjacent to the wedges. Its magnitude was also referred to the sarcolemmal surface area that was assumed to be exposed directly to Ringer's solution.

Series Resistance and Stray Capacitance

We tested the sensitivity of the data and models to the measured parameters, *RS*, the series resistance, and *CP*, the stray parallel capacitance. Fig. 7 is a plot of the measured phase angles with respect to frequency (open triangles) when fiber 3 (Table I) was mounted in the chamber. The best fit to the data by the equivalent circuit in Fig. 2 is represented by the filled circles. The open circles represent the fit of the model when *RS* was assumed to be 6,000 Ω instead of 3,905 Ω. The model did not fit the data well at the higher frequencies. The high-frequency data for this fiber showed that the maximum resistance that could have been in series with all of the capacitors in the model was between 6,000 and 6,500 Ω. If we assumed an *RS* of 6,000 Ω, the parameters that then gave the best fit to the data in Fig. 7 were: *RI* = 60 Ω cm, *CM* = 1.36 μF/cm², *RT* = 80,540 Ω cm, *CT* = 1.446 μF/cm², *RW* 8,529 Ω cm, *CW* = 0.743 μF/cm², *S* = 0.430. All parameters were different from the parameters in Table I although *RI* was altered by the greatest percentage, 75%.

The open squares in Fig. 7 represent the fit of the model when *RS* was assumed to be 2,000 Ω instead of 3,905 Ω. Again the fit is poor at higher frequencies. If we assumed an *RS* of 2,000 Ω, the parameters that gave the best fit to the data in Fig. 7 were: *RI* = 256 Ω cm, *CM* = 2.813 μF/cm², *RT* = 21,010 Ω cm, *CT* = 4.067 μF/cm², *RW* = 1,721 Ω cm, *CW* = 2.882 μF/cm², *S* = 0.806. Again, all parameters were different from those of fiber 3 in Table I. All of the capacitances were larger, and *CW* was larger by the greatest percentage, 91%.

When *CP*, the stray parallel capacitance, was assumed to be 4.0 and 0.0 pF, the data and circuit parameters were hardly altered from those observed and calculated when *CP* was 2.07 pF, the measured quantity.

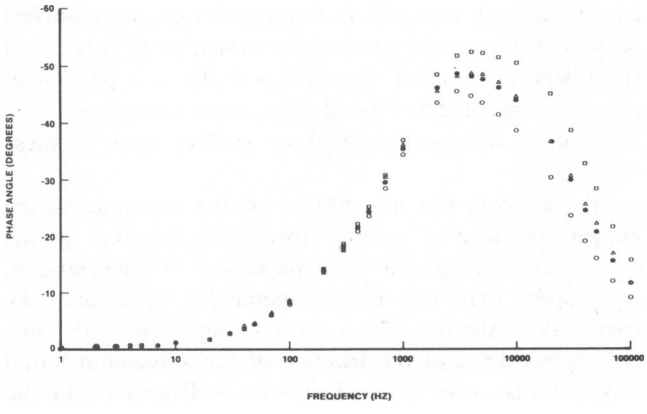

FIGURE 7 A plot of phase angle with respect to frequency for one of the fibers (fiber 3, Table I) that was mounted in the chamber and was bathed in Ringer's solution. The open triangles represent the measured data corrected for instrumental phase shift. The filled circles represent the best fit to the data by the equivalent circuit in Fig. 2 when *RS* = 3,905 Ω, as measured. The open circles and open squares represent fits to the data by the circuit in Fig. 2 when *RS* = 6,000 and 2,000 Ω, respectively.

Comparison of Equivalent Circuits with Two and Three Time Constants

Fig. 8 is a plot of the mean deviation of phase angles with respect to frequencies. The open triangles are the mean deviations between the phase data of the six fibers in Table I and the phase predictions when the equivalent circuit of the fibers had two time constants. The filled circles are the mean deviations between the phase data of the six fibers in Table I and the phase predictions when the equivalent circuit of the fibers had three time constants (Fig. 2). The stippled area is ± SEM for the deviations. The SEM that is shown at each experimental frequency was chosen from the model that had the larger SEM at that frequency. This figure shows for all six fibers what Fig. 6 shows for one fiber, i.e., that the model fiber with two branches or time constants does not fit the low-frequency points as well as does the model with three time constants. Both models give a poor fit to the data at the highest frequencies.

Fibers in Low-conductivity Solution

Fatt (1964) reported results from only one muscle in Ringer's solution. The parameters of that equivalent cir-

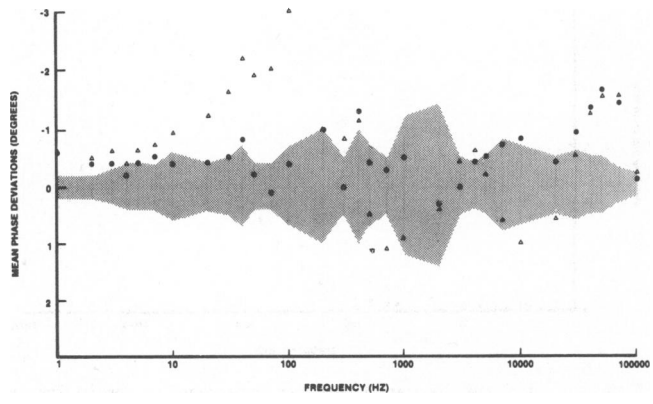

FIGURE 8 Plots of mean phase deviations of two equivalent circuits from the measured data of each of six single fibers (Table I). The open triangles are the mean deviations of the equivalent circuit in Fig. 2 without the circuit parameters *RT* and *CT*. The filled circles are the deviations of the circuit in Fig. 2. The stipled area is ± 1 SEM for the deviations.

cuit were $R_i = 227\ \Omega$ cm, $C_m = 2.14\ \mu F/cm^2$, $R_x = 13{,}300\ \Omega$ cm, and $C_x = 41.2\ \mu F/cm^2$. The preceding parameters should be compared with *RI*, *CM*, *RT*, and *CT*, respectively, from Table I. The most striking difference in the two sets of data is in C_x from Fatt (1964) and *CT* ($4.7\ \mu F/cm^2$) from Table I. Agreement was fairly good among the other parameters.

Fatt (1964) found that the low-frequency dispersion that was ascribed to R_x and C_x of his model could be studied most effectively by placing the muscles in a solution having a lesser conductivity than Ringer's solution. Table II shows the equivalent circuit parameters for two fibers bathed in a solution of low conductivity (see Methods). The single fibers were allowed to equilibrate in the low-conductivity solution for ~1 h before they were mounted for an experiment. *CT* for the two fibers (5.0 and $7.5\ \mu F/cm^2$) was again well below the magnitude of C_x found by Fatt (1964) when he used low-conductivity solutions (mean $C_x = 54\ \mu F/cm^2$ for nine muscles). The larger *RI*s in Table II compared with Table I probably indicated, as we have suggested (see Methods), that the method we used to measure *RS* was inadequate; the problems with the method were more apparent when the experiments were performed in low-conductivity solution than in Ringer's solution.

RW and *CW*

The branch of the equivalent circuit that contained *RW* and *CW* was assumed to result from the experimental arrangement of fiber and insulating wedges such that part of the capacitance of the sarcolemma was in series with the shunt resistance around the fiber. We suspected that the lowest shunt resistance was located near the uppermost and lowermost parts of the segment within the disk where the upper and lower parts of the wedges formed a corner between the segment of fiber and the inner surfaces of the disk. If our suspicions were correct, they explain why *CW* was never greater than *CM* even though the parameter *S* indicated that it should have been. If the parameter *S* had the physical significance suggested in Fig. 3, then its magnitude (Tables I and II) indicated that more sarcolemmal surface area touched the wedges than was exposed directly to the bathing solution.

On two occasions we attempted to test glycerol-treated fibers (Howell, 1969; Eisenberg et al., 1971) in an effort to determine whether access to *RW* and *CW* depended upon the transverse tubular system. Unfortunately, the single glycerol-treated fibers did not survive being pulled through the silicone rubber seals in the disk (see Methods). As an alternative test of whether access to *RW* and *CW* depended upon *RT* and *CT*, we fit the data from all fibers to an equivalent circuit in which *RW* and *CW* formed a branch in parallel with *CT*. We thought that if *RW* and *CW* were in fact properties of sarcoplasmic reticulum and not artifacts as suggested, then the new circuit might be more realistic than the circuit in Fig. 2. The mean best-fit parameters in the new circuit were: $RI = 218\ \Omega$ cm; $CM = 2.215\ \mu F/cm^2$; $RT = 2{,}595\ \Omega$ cm; $CT = 2.005\ \mu F/cm^2$; $RW = 23{,}807\ \Omega$ cm; $CW = 4.226\ \mu F/cm^2$; $S = 0.694$. The magnitudes of *RT* and *CT* in this circuit are approximately equal to the magnitudes of *RW* and *CW* in Table I and vice versa. Again, no capacitance of $50\ \mu F/cm^2$ was fit. Although it might be interesting to speculate about how the sarcoplasmic reticulum and transverse tubular system could result in capacitances of 4.226 and 2.005 $\mu F/cm^2$, respectively, a circuit in which *RT* is only 2,595 Ω cm would be difficult to justify; it would correspond to a model-dependent specific resistance, usually represented as R_c, of only 17 $\Omega\ cm^2$

$$\left[R_c = \frac{RI \cdot (1 + S) \cdot \pi \cdot \text{Diam}}{8}\right].$$

DISCUSSION

We measured the transverse impedance of single muscle fibers to see if an equivalent circuit that provided the best fit to the data would contain a capacitance large enough that it could be attributed to the membranes of the transverse tubular system and sarcoplasmic reticulum. Our reason for thinking that these experiments might reveal the electrical properties of the sarcoplasmic reticulum was based on the results of Fatt (1964). Fatt investigated the transverse impedance of whole sartorius muscles and fit those data with an equivalent circuit that included a capacitance that was sufficiently large that it could be ascribed to the transverse tubular system and sarcoplasmic reticulum of the fibers. Fatt proposed three possibilities for R_x and C_x: (*a*) properties of a system of channels that transverse the fibers (sarcotubular system and access resistance); (*b*) consequence of the passage of current in an

TABLE II
PARAMETERS OF AN EQUIVALENT CIRCUIT OF SINGLE MUSCLE FIBERS IN A LOW CONDUCTIVITY SOLUTION

Fiber	Diameter*	*RI*	*CM*‡	*RT*	*CT*‡	*RW*	*CW*‡	*S*	*RP**
	(microns)	*(Ω cm)*	*(μF/cm²)*	*(Ω cm)*	*(μF/cm²)*	*(Ω cm)*	*(μF/cm²)*		*(Ω)*
1	118	2,030	1.528	231,800	4.952	75,670	0.750	0.686	368,300
2	90	3,543	1.663	200,800	7.496	51,340	0.970	0.781	545,500

*Diameter and RP were measured quantities.
‡Referred to the surface area of the part of the segments that was directly exposed to solution.

adsorbed layer of ions immediately outside the fibers; (*c*) nonlinear and active electrical behavior of the fibers.

The equivalent circuit that we used to describe the impedance of the fibers had three branches, and each branch included a resistance and a capacitance in series. One branch, which had the intermediate time constant of the three branches, was concluded to be caused by the unique experimental arrangement that we used to measure the impedance. We reached that conclusion because the physical arrangement of the experimental apparatus made it a possibility that had to be considered, the magnitudes of *RW* and *CW* were not suggestive of membranous structures in muscle fibers, and numerous investigations of the passive electrical properties of muscle at frequencies >1 Hz have revealed only two time constants in the equivalent circuit.

Another branch, which had the smallest time constant, was caused by the resistance of the cytoplasm and the capacitance of the sarcolemmal membrane. There was very good agreement between those parameters and the results of Fatt (1964) and others. The third branch of the circuit had the largest time constant of the three branches, but it was not as large as the time constant that was determined by Fatt. The major difference in the two sets of data was in the magnitudes of the capacitances C_x and *CT* (mean $C_x = 54\ \mu F/cm^2$, $n = 9$ muscles in low conductivity solution, Fatt, 1964; mean $CT = 4.7\ \mu F/cm^2$, $n = 6$ single fibers in Ringer's solution, Table I). *CT* is consistent with the magnitude one would expect and that has been measured and suggested to represent the capacitance of the membranes of the transverse tubular system (Falk and Fatt, 1964; Freygang et al., 1967; Schneider, 1970; Valdiosera et al., 1974*b*) whereas C_x is consistent with the magnitude that one would expect for the capacitance of the membranes of the sarcoplasmic reticulum. Our conclusion is that current did not get into the sarcoplasmic reticulum in the single muscle fibers that we studied.

We must point out that the magnitude of *CT*, which we believe represents the electrical properties of the transverse tubular system, is subject to the arbitrary assumption that the fraction of transverse tubular membranes that become charged is proportional to the fraction of the sarcolemmal surface that is exposed directly to Ringer's solution, i.e., in our model *CT* is determined by the factor $(1 - S)$. If in fact all or a very large fraction of the tubular system was charged during these experiments, then the magnitude of *CT* determined from the fit would be $<4.7\ \mu F/cm^2$.

We think that the lumped model that we used in this study was adequate and appropriate for comparing our results with those of Fatt (1964). A different model that would have incorporated the distributed property of the transverse tubular resistance and capacitance, the distributed property of the series resistance, the shunt resistance, and the sarcolemmal capacitance in our experiments might have been necessary if we had found evidence that current did get into the sarcoplasmic reticulum. We also could have eliminated *RI* as an adjustable parameter in the model by simply eliminating its effects along with the membrane and shunt resistances (*RP*, Fig. 2). However, because we wanted to obtain a measurement of *RI* in series with *CM*, we allowed *RI* to be an implicit part of *RP*, *RT*, and *RW*, as noted earlier.

We suspect that the primary reason for the difference in the magnitudes of *CT* in Table I and C_x from Fatt (1964) was not due to the different methods of obtaining the data on impedance but in the methods of fitting the models to the data. The methods of nonlinear curve fitting by the least-squares criterion were not available to Fatt in 1964. Before we incorporated the compression factor, *S*, and the third branch, *RT* and *CT*, into our model, a guess of 50 $\mu F/cm^2$ given to the computer for *CW* did indeed result in convergence to a best least-squares fit with a *CW* of ~50 $\mu F/cm^2$. However, a comparison of phase plots of the data from the model and the experimental data showed that the model did not describe the experimental data very well.

Fig. 9 is the result of an effort to compare our results with the results of Fatt (1964). The open triangles represent our data for fiber 5 (Table I), which was mounted in the chamber and bathed in Ringer's solution. The filled circles represent the best fit to the data by the model in Fig. 2. The open squares represent a plot from the model in Fig. 2 using the best-fit parameters for fiber 5 except $RT = 13{,}300\ \Omega$ cm and $CT = 41.2\ \mu F/cm^2$; i.e., Fatt's results for R_x and C_x in Ringer's solution were substituted for the parameters *RT* and *CT* that were chosen by the computer. Fiber 5 was chosen for the comparison because that fiber probably experienced the largest degree of shunting of all six fibers, and therefore we expected that the two fits to the data would differ the least in absolute terms for fiber 5 than for any of the other fibers. Fig. 9 shows that substitution of R_x and C_x for *RT* and *CT* in the model gives a poor fit to the data between 10 and 10,000 Hz, whereas a good fit is obtained between 10,000 and 100,000 Hz.

An alternative method of comparison was to fix *RT* and

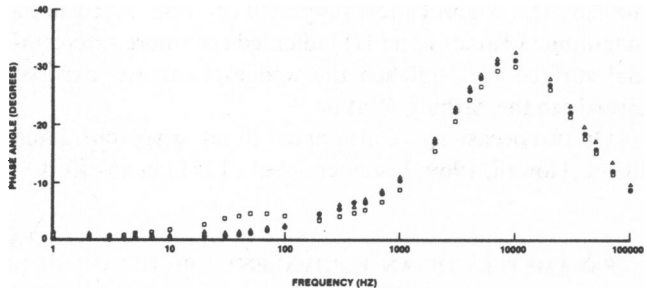

FIGURE 9 A plot of phase angle with respect to frequency for one of the fibers (fiber 5, Table I) that was mounted in the chamber and was bathed in Ringer's solution. The open triangles represent the measured data corrected for instrumental phase shift. The filled circles represent the best fit to the data by the equivalent circuit in Fig. 2. The open squares represent the fit to the data by the circuit in Fig. 2 when $RT = 13{,}300\ \Omega$ cm and $CT = 41.2\ \mu F/cm^2$.

CT at 13,300 Ω cm and 41.2 $\mu F/cm^2$, respectively, and allow only RI, CM, RW, CW, and S to be fit to the data. In that case the best fit parameters were RI = 47.6 Ω cm, CM = 7.6 $\mu F/cm^2$, RW = 1,733 Ω cm, CW = 3.17 $\mu F/cm^2$, and S = 0.847. This latter model, which gives a somewhat better fit for the Fatt parameters, still gives a significantly poorer fit at the 5% level from the model that incorporated the parameters that are given in Table I.

We thank Dr. Walter Freygang for many valuable discussions on this project. We would like to thank Dr. Chris Clausen, who gave us the computer programs for curve fitting, and Dr. Lowell Stone, who read the manuscript. Messrs. Nicholas Ricchiuti, Carl Vette, and Kenny Teoh kindly provided technical advice.

This work was supported by Established Investigatorship 75-205 from the American Heart Association, and grants PCM77-17693 and PCM79-19087 from the National Science Foundation.

Received for publication 2 November 1981 and in revised form 18 March 1982.

REFERENCES

Clausen, C., S. A. Lewis, and J. M. Diamond. 1979. Impedance analysis of a tight epithelium using a distributed resistance model. *Biophys. J.* 26:291–318.

Cole, K. S. 1968. Membranes, Ions and Impulses. University of California Press. 12.

Eisenberg, R. S., J. N. Howell, and P. C. Vaughan. 1971. The maintenance of resting potentials in glycerol-treated muscle fibers. *J. Physiol. (Lond.)*. 215:95–102.

Falk, G., and P. Fatt. 1964. Linear electrical properties of striated muscle fibers observed with intracellular electrodes. *Proc. R. Soc. B. Biol. Sci.* 160:69–123.

Fatt, P. 1964. An analysis of the transverse electrical impedance of striated muscle. *Proc. R. Soc. B. Biol. Sci.* 159:606–651.

Freygang, W. H., Jr., S. I. Rapoport, and L. D. Peachey. 1967. Some relations between changes in the linear electrical properties of striated muscle fibers and changes in ultrastructure. *J. Gen. Physiol.* 50:2437–2458.

Howell, J. N. 1969. A lesion of the transverse tubules of skeletal muscle. *J. Physiol. (Lond.)*. 201:515–533.

Mobley, B. A., and B. R. Eisenberg. 1975. Sizes of components in frog skeletal muscle measured by methods of stereology. *J. Gen. Physiol.* 66:31–45.

Mobley, B. A., J. Leung, and R. S. Eisenberg. 1975. Longitudinal impedance of single frog muscle fibers. *J. Gen. Physiol.* 65:97–113.

Peachey, L. D. 1965. The sarcoplasmic reticulum and transverse tubules of the frog's sartorius. *J. Cell Biol.* 25:209–231.

Schneider, M. F. 1970. Linear electrical properties of the transverse tubules and surface membrane of skeletal muscle fibers. *J. Gen. Physiol.* 56:640–671.

Valdiosera, R., C. Clausen, and R. S. Eisenberg. 1974 *a*. Circuit models of the passive electrical properties of frog skeletal muscle fibers. *J. Gen. Physiol.* 63:432–459.

Valdiosera, R., C. Clausen, and R. S. Eisenberg. 1974 *b*. Impedance of frog skeletal muscle fibers in various solutions. *J. Gen. Physiol.* 63:460–491.